Available online at www.sciencedirect.com
SCIENCE DIRECT
ELSEVIER
Journal of Sound and Vibration 279 (2005) 497–507
JOURNAL OF SOUND AND VIBRATION
www.elsevier.com/locate/jsvi

Short Communication

Analysis of a fluid-loaded thick plate

Andrew J. Hull

Weapons Technology and Undersea Systems Department, Naval Undersea Warfare Center Division, Newport, RI 02841, USA

Received 25 November 2002; accepted 6 January 2004
Available online 1 October 2004

1. Introduction

Central to the study and understanding of slab-shaped material motion is plate theory, which has been researched extensively for many years. Thin plate theory [1] is a simplified version that fails to accurately incorporate dynamic response when the sample is thick compared to a wavelength. In contrast, thick plate theory [2] usually incorporates all the dynamics of the plate and is normally used when the sample is on the order of a wavelength of energy in the structure. More complex investigations have analyzed the dispersion curve for the plate without fluid loading [3–5] or for the plate in contact with a continuous fluid on one or both sides [6–11]. Additional papers have been published that examine plate response to various other loading configurations. For example, studies have explored the radiation efficiency of infinite fluid-loaded plates subjected to point loads [12], calculated the corresponding transfer functions for thin plate models coupled to fluid loading [13], and determined mode shapes for a thick plate with finite depth that is loaded by fluid on both sides [14]. Multilayer theory has also been developed for this problem [15]. During these investigations, the response of thick-walled plates has been typically left as an open-form solution that involves a matrix inverse at a specific wavenumber and frequency.

This paper derives the equations of motion of an infinite, isotropic thick plate, either not in contact with fluid, or coupled on one or both sides with fluid loading as it is excited with a continuous plane wave forcing function. The equations of motion are formulated into a four-by-four system of linear equations with four-wave propagation coefficients as the unknown terms.

E-mail address: hullaj@npt.nuwc.navy.mil (A.J. Hull).

doi:10.1016/j.jsv.2004.01.051

Once the system matrix is known, the dispersion equations, derived in closed-form expressions from the determinant of the matrix, explicitly show the effects of the fluid loading. Calculated next are the closed-form transfer functions of plate motion divided by source excitation, which are written in a form that expresses the plate and the fluid terms separately. Based on these transfer functions, the displacement shapes of the plate modes are studied with respect to the unloaded plate and fluid loading on one or both sides of the plate.

2. System model

The system model is a thick plate in contact on none, one, or both sides with a fluid that exerts a continuous pressure on the plate. In the case of the plate without fluid, the force on the plate is a mechanical force applied directly to the plate. The model configurations, referred to as nonfluid-loaded, single fluid-loaded, and double fluid-loaded plates, are based on the following assumptions: (1) the forcing function acting on the plate is a plane wave with definite wavenumber and frequency content, (2) the corresponding response of the plate is at a definite wavenumber and frequency, (3) motion is normal and tangential to the plate in one direction (two-dimensional system), (4) the plate has an infinite spatial extent, (5) the particle motion and pressure response is linear, and (6) the fluid medium, when present, has no loss. For the case where the fluid is on both sides of the plate, each fluid has the same acoustic properties.

The motion of the plate for all cases is governed by the equation [16]

$$\mu\nabla^2\mathbf{u} + (\lambda + \mu)\nabla\nabla\bullet\mathbf{u} = \rho\frac{\partial^2\mathbf{u}}{\partial t^2}, \tag{1}$$

where ρ is the density (kg/m^3), λ and μ are the Lamé constants (N/m^2), t is the time (s), $\bullet$ denotes a vector dot product, and $\mathbf{u}$ is the Cartesian coordinate displacement vector of the plate. The coordinate system of the plate is shown in Fig. 1. Note that the use of this orientation results in $b = 0$ and a having a value less than zero. Furthermore, the thickness of the plate, h, is a positive value. For the single and double fluid-loaded plates, the acoustic pressure in the fluid on the excitation side of the plate is governed by the wave equation and is written in Cartesian coordinates as [17]

$$\frac{\partial^2 p_1(x,z,t)}{\partial z^2} + \frac{\partial^2 p_1(x,z,t)}{\partial x^2} - \frac{1}{c_f^2}\frac{\partial^2 p_1(x,z,t)}{\partial t^2} = 0, \tag{2}$$

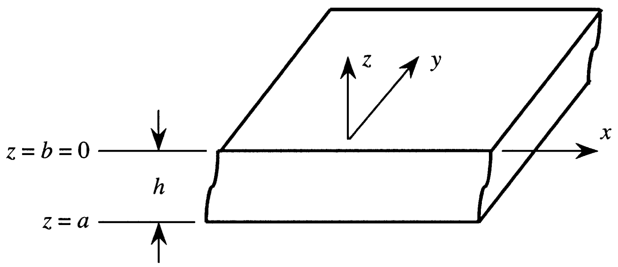

Fig. 1. Coordinate system used in model.

where $p_1(x,z,t)$ is the pressure (N/m^2), with subscript 1 denoting the fluid on the excitation side of the plate; z is the spatial location (m) normal to the plate, x is the spatial location (m) tangential to the plate, and c_f is the compressional wave speed of the fluid (m/s). For the double fluid-loaded plate, the acoustic pressure in the fluid opposite the excitation side of the plate is governed by the wave equation and is written in Cartesian coordinates as

$$\frac{\partial^2 p_2(x,z,t)}{\partial z^2} + \frac{\partial^2 p_2(x,z,t)}{\partial x^2} - \frac{1}{c_f^2}\frac{\partial^2 p_2(x,z,t)}{\partial t^2} = 0, \tag{3}$$

where $p_2(x,z,t)$ is the pressure (N/m^2) and subscript 2 denotes the fluid opposite the excitation side of the plate. The above equations are the governing partial differential equations of the nonfluid-loaded, single fluid-loaded and double fluid-loaded plate systems.

Eqs. (1)–(3) are coupled to each other using four to six boundary conditions, depending on the presence or absence of fluid. The normal stress at the top of the plate ($z = b$) is equal to the opposite of the pressure in the fluid and is expressed as

$$\tau_{zz}(x,b,t) = (\lambda + 2\mu)\frac{\partial u_z(x,b,t)}{\partial z} + \lambda\frac{\partial u_x(x,b,t)}{\partial x} = -p_1(x,b,t), \tag{4}$$

where $u_z(x,z,t)$ is the displacement in the z-direction (m) and $u_x(x,z,t)$ is the displacement in the x-direction (m). The tangential stress at the top of the plate is zero and is written as

$$\tau_{zx}(x,b,t) = \mu\left[\frac{\partial u_x(x,b,t)}{\partial z} + \frac{\partial u_z(x,b,t)}{\partial x}\right] = 0. \tag{5}$$

For the double fluid-loaded plate, the normal stress at the bottom of the plate ($z = a$) is equal to the opposite of the pressure in the fluid. This expression is

$$\tau_{zz}(x,a,t) = (\lambda + 2\mu)\frac{\partial u_z(x,a,t)}{\partial z} + \lambda\frac{\partial u_x(x,a,t)}{\partial x} = -p_2(x,a,t), \tag{6}$$

where $p_2(x,a,t)$ represents the transmitted (or radiated) acoustic pressure in the fluid field on the opposite side of the acoustic excitation. For the nonfluid-loaded and single fluid-loaded plate, $p_2(x,z,t) \equiv 0$ in Eq. (6). The tangential stress at the bottom of the plate is zero, with this equation written as

$$\tau_{zx}(x,a,t) = \mu\left[\frac{\partial u_x(x,a,t)}{\partial z} + \frac{\partial u_z(x,a,t)}{\partial x}\right] = 0. \tag{7}$$

For the single and double fluid-loaded plates, the interface between the first fluid and the surface of the plate at $z = b$ satisfies the linear momentum equation, which is [18]

$$\rho_f\frac{\partial^2 u_z(x,b,t)}{\partial t^2} = -\frac{\partial p_1(x,b,t)}{\partial z}, \tag{8}$$

where ρ_f is the density of the fluid (kg/m^3). For the double fluid-loaded plate, the interface between the second fluid and the surface of the plate at $z = a$ also satisfies the linear momentum equation and is written as

$$\rho_f\frac{\partial^2 u_z(x,a,t)}{\partial t^2} = -\frac{\partial p_2(x,a,t)}{\partial z}. \tag{9}$$

Modeling the displacement as a dilatational wave and a shear wave, and inserting this term into Eqs. (1)–(9), results in the plate displacements given by

$$\begin{aligned} u_x(x,z,t) &= U_x(k_x,z,\omega)\ \exp(\mathrm{i}k_x x)\ \exp(\mathrm{i}\omega t) \\ &= [A(k_x,\omega)\mathrm{i}k_x\ \exp(\mathrm{i}\alpha z) + B(k_x,\omega)\mathrm{i}k_x\ \exp(-\mathrm{i}\alpha z) \\ &\quad - C(k_x,\omega)\mathrm{i}\beta\ \exp(\mathrm{i}\beta z) + D(k_x,\omega)\mathrm{i}\beta\ \exp(-\mathrm{i}\beta z)] \\ &\quad \times \exp(\mathrm{i}k_x x)\exp(\mathrm{i}\omega t) \end{aligned} \tag{10}$$

and

$$\begin{aligned} u_z(x,z,t) &= U_z(k_x,z,\omega)\ \exp(\mathrm{i}k_x x)\ \exp(\mathrm{i}\omega t) \\ &= [A(k_x,\omega)\mathrm{i}\alpha\ \exp(\mathrm{i}\alpha z) - B(k_x,\omega)\mathrm{i}\alpha\ \exp(-\mathrm{i}\alpha z) \\ &\quad + C(k_x,\omega)\mathrm{i}k_x\ \exp(\mathrm{i}\beta z) + D(k_x,\omega)\mathrm{i}k_x\ \exp(-\mathrm{i}\beta z)] \\ &\quad \times \exp(\mathrm{i}k_x x)\ \exp(\mathrm{i}\omega t), \end{aligned} \tag{11}$$

where $A(k_x,\omega), B(k_x,\omega), C(k_x,\omega)$, and $D(k_x,\omega)$ are wave propagation constants of the plate and are determined by solving the four by four system described below; $\mathrm{i} = \sqrt{-1}$; ω is frequency (rad/s); α is the modified wavenumber associated with the dilatational wave and is expressed as

$$\alpha = \sqrt{k_d^2 - k_x^2}, \tag{12}$$

where k_d is the dilatational wavenumber and is equal to ω/c_d where c_d is the dilatational wave speed (m/s); β is the modified wavenumber (rad/m) associated with the shear wave and is expressed as

$$\beta = \sqrt{k_s^2 - k_x^2}, \tag{13}$$

where k_s is the shear wavenumber (rad/m) and is equal to ω/c_s where c_s is the shear wave speed (m/s); and k_x is the spatial wavenumber in the x-direction (rad/m). If the pressure in the fluid is generated by an acoustic plane wave, the spatial wavenumber is given by

$$k_x = \frac{\omega}{c_f}\sin(\theta), \tag{14}$$

where θ is the angle of incidence (rad) of the incoming acoustic wave, with $\theta = 0$ corresponding to excitation normal to the plate (or broadside excitation). Wavenumbers larger than ω/c_f are possible and are typically generated from turbulent fluid loading or structural wave loading. The relationship between the wave speeds c_d and c_s and the Lamé constants are determined by

$$c_d = \sqrt{\frac{\lambda + 2\mu}{\rho}}, \qquad c_s = \sqrt{\frac{\mu}{\rho}}. \tag{15,16}$$

Assembling Eqs. (1)–(16) yields the four-by-four system of linear equations that model the system:

$$\mathbf{Ax} = \mathbf{b}, \tag{17}$$

where the entries of Eq. (17) are

$$A_{11p} = -\alpha^2\lambda - 2\alpha^2\mu - \lambda k_x^2, \qquad A_{11s} = A_{11d} = \frac{\rho_f \omega^2 \alpha}{\gamma}, \tag{18,19}$$

$$A_{11} = A_{11p} + A_{11s}, \qquad A_{12} = A_{11p} - A_{11s}, \qquad A_{13p} = 2k_x\beta\mu, \tag{20−22}$$

$$A_{13s} = A_{13d} = \frac{\rho_f \omega^2 k_x}{\gamma}, \qquad A_{13} = -A_{13p} + A_{13s}, \qquad A_{14} = A_{13p} + A_{13s}, \tag{23−25}$$

$$A_{21} = -2\mu k_x \alpha, \qquad A_{22} = -A_{21}, \qquad A_{23} = \mu\beta^2 - \mu k_x^2, \qquad A_{24} = A_{23}, \tag{26−29}$$

$$\begin{aligned} &A_{31} = (A_{11p} - A_{11d})\ \exp(\mathrm{i}\alpha a), \qquad A_{32} = (A_{11p} + A_{11d})\exp(-\mathrm{i}\alpha a), \\ &A_{33} = (-A_{13p} - A_{13d})\ \exp(\mathrm{i}\beta a), \end{aligned} \tag{30−32}$$

$$\begin{aligned} &A_{34} = (A_{13p} - A_{13d})\ \exp(-\mathrm{i}\beta a), \qquad A_{41} = A_{21}\ \exp(\mathrm{i}\alpha a), \\ &A_{42} = -A_{21}\ \exp(-\mathrm{i}\alpha a), \end{aligned} \tag{33−35}$$

$$A_{43} = A_{23}\ \exp(\mathrm{i}\beta a), \qquad A_{44} = A_{23}\ \exp(-\mathrm{i}\beta a), \tag{36,37}$$

$$\begin{aligned} &x_{11} = A(k_x, \omega), \qquad x_{21} = B(k_x, \omega), \\ &x_{31} = C(k_x, \omega), \qquad x_{41} = D(k_x, \omega) \end{aligned} \tag{38−41}$$

$$b_{11p} = -P_e(\omega), \qquad b_{11s} = -P_e(\omega), \tag{42,43}$$

$$b_{11} = b_{11p} + b_{11s}, \qquad b_{21} = 0, \qquad b_{31} = 0, \qquad b_{41} = 0. \tag{44−47}$$

In Eqs. (19) and (23),

$$\gamma = \sqrt{\left(\frac{\omega}{c_f}\right)^2 - k_x^2}, \tag{48}$$

where γ is the wavenumber of the acoustic pressure in the fluid (rad/m). In Eqs. (42) and (43), $P_e(\omega)$ is the excitation level of the incoming energy. In Eqs. (18)–(47), subscript p corresponds to terms related to the plate, subscript s corresponds to the case of both the single and double fluid-loaded plates, and subscript d corresponds only to the case of the double fluid-loaded plate. To model the behavior of the thick plate without the fluid loads, the terms with subscripts s and d are set equal to zero. To model the behavior of the fluid plate with a single fluid load, the terms with the subscript d are set equal to zero.

3. Dispersion equations

The dispersion equation is an equation whose zeros correspond to single-mode propagation in the structure. This function is proportional to the determinant of **A** in Eq. (17). For the case of the nonfluid-loaded plate, the determinant of **A** is calculated in closed form and is written as

$$\Delta_n(k_x,\omega) = p_1(k_x,\omega)\cos(\alpha h)\,\cos(\beta h) + p_2(k_x,\omega)\sin(\alpha h)\sin(\beta h) - p_1(k_x,\omega), \tag{49}$$

where

$$p_1(k_x,\omega) = -8\alpha\beta k_x^2(\beta^2 - k_x^2)^2 \tag{50}$$

and

$$p_2(k_x,\omega) = (\beta^2 - k_x^2)^4 + 16\alpha^2\beta^2 k_x^4. \tag{51}$$

For the case of the single fluid-loaded plate, the determinant of **A** is written as

$$\begin{aligned}\Delta_s(k_x,\omega) = {} & p_1(k_x,\omega)\cos(\alpha h)\cos(\beta h) + f_1(k_x,\omega)\cos(\alpha h)\sin(\beta h) \\ & + f_2(k_x,\omega)\sin(\alpha h)\cos(\beta h) + p_2(k_x,\omega)\sin(\alpha h)\sin(\beta h) \\ & - p_1(k_x,\omega),\end{aligned} \tag{52}$$

where

$$f_1(k_x,\omega) = \mathrm{i}\rho_f(\gamma\rho)^{-1}\alpha(\beta^2 - k_x^2)^2(\beta^2 + k_x^2)^2 \tag{53}$$

and

$$f_2(k_x,\omega) = 4\mathrm{i}\rho_f(\gamma\rho)^{-1}\alpha^2\beta k_x^2(\beta^2 + k_x^2)^2. \tag{54}$$

For the case of the double fluid-loaded plate, the determinant of **A** is written as

$$\begin{aligned}\Delta_d(k_x,\omega) = {} & p_1(k_x,\omega)\cos(\alpha h)\cos(\beta h) + 2f_1(k_x,\omega)\cos(\alpha h)\sin(\beta h) \\ & + 2f_2(k_x,\omega)\sin(\alpha h)\cos(\beta h) \\ & + [p_2(k_x,\omega) + f_3(k_x,\omega)]\sin(\alpha h)\sin(\beta h) - p_1(k_x,\omega),\end{aligned} \tag{55}$$

where

$$f_3(k_x,\omega) = \rho_f^2(\gamma\rho)^{-2}\alpha^2(\beta^2 + k_x^2)^4. \tag{56}$$

In Eqs. (49), (52), and (55), the p constants corresponds to terms associated with the plate and the f constants correspond to terms associated with the fluid loads.

It is noted that these dispersion curves without the fluid load and with the double fluid load have both been previously derived. The plate dispersion curve without fluid loading is known as the Rayleigh–Lamb frequency equation for the propagation of waves in a plate, which is given in Ref. [19] as Eq. (8.1.61). The plate dispersion curve with the double fluid load for the case of symmetrical wave response is listed in Ref. [6] as Eq. (25) and for the case of antisymmetrical response is shown as Eq. (26). Eqs. (49) and (55), although not identical to those listed in Refs. [19,6], have the same zeros that correspond to the branches of the dispersion curves for the nonfluid-loaded and double fluid-loaded plate.

4. Closed-form transfer functions

The closed-form transfer functions can be determined by solving Eq. (17) as

$$\mathbf{x} = \mathbf{A}^{-1}\mathbf{b}, \tag{57}$$

then taking the entries of $\mathbf{x}$ and inserting them into Eqs. (10) and (11), and finally reducing the resultant expressions. For the nonfluid-loaded plate, the transfer function of the tangential displacement at location z divided by the excitation level is equal to

$$\frac{U_x^{(n)}(k_x, z, \omega)}{P_e(\omega)} = \frac{U_x^{(Tn)}(k_x, z, \omega)}{2\mu\Delta_n(k_x, \omega)}, \tag{58}$$

where

$$\begin{aligned} U_x^{(Tn)}(k_x, z, \omega) = {} & p_3\{\cos(\alpha z) - \cos(\beta h)\cos[\alpha(z+h)]\} \\ & + p_4\{\cos(\beta z) - \cos(\alpha h)\cos[\beta(z+h)]\} \\ & + p_5 \sin(\alpha h)\sin[\beta(z+h)] + p_6\sin(\beta h)\sin[\alpha(z+h)] \end{aligned} \tag{59}$$

with

$$p_3(k_x, \omega) = 8\mathrm{i}\alpha\beta k_x^3(\beta^2 - k_x^2), \qquad p_4(k_x, \omega) = -4\mathrm{i}\alpha\beta k_x(\beta^2 - k_x^2)^2, \tag{60,61}$$

$$p_5(k_x, \omega) = -16\mathrm{i}\alpha^2\beta^2 k_x^3, \qquad p_6(k_x, \omega) = 2\mathrm{i}k_x(\beta^2 - k_x^2)^3. \tag{62,63}$$

For the single fluid-loaded plate, the transfer function of the tangential displacement at location z divided by the excitation level is equal to

$$\frac{U_x^{(s)}(k_x, z, \omega)}{P_e(\omega)} = \frac{U_x^{(Tn)}(k_x, z, \omega)}{\mu\Delta_s(k_x, \omega)}. \tag{64}$$

For the double fluid-loaded plate, the transfer function of the tangential displacement at location z divided by the excitation level is equal to

$$\frac{U_x^{(d)}(k_x, z, \omega)}{P_e(\omega)} = \frac{U_x^{(Td)}(k_x, z, \omega)}{\mu\Delta_d(k_x, \omega)}, \tag{65}$$

where

$$\begin{aligned} U_x^{(Td)}(k_x, z, \omega) = {} & p_3\{\cos(\alpha z) - \cos(\beta h)\cos[\alpha(z+h)]\} \\ & + p_4\{\cos(\beta z) - \cos(\alpha h)\cos[\beta(z+h)]\} \\ & + p_5 \sin(\alpha h)\sin[\beta(z+h)] + p_6\sin(\beta h)\sin[\alpha(z+h)] \\ & + f_4 \sin(\alpha h)\cos[\beta(z+h)] + f_5\sin(\beta h)\cos[\alpha(z+h)] \end{aligned} \tag{66}$$

with

$$f_4(k_x, \omega) = 4\rho_f(\gamma\rho)^{-1}\alpha^2\beta k_x(\beta^2 + k_x^2)^2 \tag{67}$$

and

$$f_5(k_x, \omega) = -2\rho_f(\gamma\rho)^{-1}\alpha k_x(\beta^2 - k_x^2)(\beta^2 + k_x^2)^2. \tag{68}$$

For the nonfluid-loaded plate, the transfer function of the normal displacement at location z divided by the excitation level is equal to

$$\frac{U_z^{(n)}(k_x, z, \omega)}{P_e(\omega)} = \frac{U_z^{(Tn)}(k_x, z, \omega)}{2\mu\Delta_n(k_x, \omega)}, \tag{69}$$

where

$$\begin{aligned} U_z^{(Tn)}(k_x, z, \omega) = {} & p_7\{\sin(\alpha z) - \cos(\beta h)\sin[\alpha(z+h)]\} \\ & + p_8\{\sin(\beta z) - \cos(\alpha h)\sin[\beta(z+h)]\} \\ & + p_9 \sin(\alpha h)\cos[\beta(z+h)] + p_{10}\sin(\beta h)\cos[\alpha(z+h)] \end{aligned} \tag{70}$$

with

$$p_7(k_x, \omega) = -8\alpha^2\beta k_x^2(\beta^2 - k_x^2), \qquad p_8(k_x, \omega) = -4\alpha k_x^2(\beta^2 - k_x^2)^2, \tag{71,72}$$

$$p_9(k_x, \omega) = 16\alpha^2\beta k_x^4, \quad p_{10}(k_x, \omega) = 2\alpha(\beta^2 - k_x^2)^3. \tag{73,74}$$

For the single fluid-loaded plate, the transfer function of the normal displacement at location z divided by the excitation level is equal to

$$\frac{U_z^{(s)}(k_x, z, \omega)}{P_e(\omega)} = \frac{U_z^{(Tn)}(k_x, z, \omega)}{\mu\Delta_s(k_x, \omega)}. \tag{75}$$

For the double fluid-loaded plate, the transfer function of the normal displacement at location z divided by the excitation level is equal to

$$\frac{U_z^{(d)}(k_x, z, \omega)}{P_e(\omega)} = \frac{U_z^{(Td)}(k_x, z, \omega)}{\mu\Delta_d(k_x, \omega)}, \tag{76}$$

where

$$\begin{aligned} U_z^{(Td)}(k_x, z, \omega) = {} & p_7\{\sin(\alpha z) - \cos(\beta h)\sin[\alpha(z+h)]\} \\ & + p_8\{\sin(\beta z) - \cos(\alpha h)\sin[\beta(z+h)]\} \\ & + p_9 \sin(\alpha h)\cos[\beta(z+h)] + p_{10}\sin(\beta h)\cos[\alpha(z+h)] \\ & + f_6 \sin(\alpha h)\sin[\beta(z+h)] + f_7\sin(\beta h)\sin[\alpha(z+h)] \end{aligned} \tag{77}$$

with

$$f_6(k_x, \omega) = -4\mathrm{i}\rho_f(\gamma\rho)^{-1}\alpha^2 k_x^2(\beta^2 + k_x^2)^2 \tag{78}$$

and

$$f_7(k_x, \omega) = -2\mathrm{i}\rho_f(\gamma\rho)^{-1}\alpha^2(\beta^2 - k_x^2)(\beta^2 + k_x^2)^2. \tag{79}$$

5. Displacement shapes

A numerical example is discussed to illustrate the effects of fluid loading on the displacement shapes of the plate. A baseline problem is defined that corresponds to a mildly stiff elastomeric solid in contact with sea water on one or two sides. The plate material properties are as follows: Young's modulus is $E = 10^8\ \mathrm{N/m^2}$, density is $\rho = 1200\ \mathrm{kg/m^3}$, Poisson's ratio is $v = 0.4$ (dimensionless), and thickness is $h = 0.1\ \mathrm{m}$. The sea water has a compressional wave speed of $c_f = 1500\ \mathrm{m/s}$ and a density of $\rho_f = 1025\ \mathrm{kg/m^3}$. The calculated Lamé constants are $\lambda = 1.43 \times 10^8\ \mathrm{N/m^2}$ and $\mu = 3.57 \times 10^7\ \mathrm{N/m^2}$. The calculated dilatational wave speed is $c_d = 423\ \mathrm{m/s}$ and the calculated shear wave speed is $c_s = 173\ \mathrm{m/s}$. The dispersion curves for the system are not plotted as they are previously available using other work [6,19], nor are the transfer functions because they are previously available as open form solutions [19] which match identically the closed-form solutions derived in the previous section.

Fig. 2 shows the displacement shape of the $n = 1$ antisymmetric mode for the nonfluid-loaded plate, the single fluid-loaded plate, and the double fluid-loaded plate. The figure on the left illustrates plate thickness versus tangential displacement and the figure on the right shows plate thickness versus normal displacement. The solid line is the double fluid-loaded plate, and the dashed line represents both the nonfluid-loaded plate and the single fluid-loaded plate. The displacement shapes were determined by taking a point on the $n = 1$ branch of each dispersion curve for the three separate cases and then using these values of frequency and wavenumber to compute the displacements. For the double fluid-loaded plate, the values of this point were $f = 2540\ \mathrm{Hz}$ and $k_x = 78.5\ \mathrm{rad/m}$; for the single fluid-loaded plate, these values were $f = 2630\ \mathrm{Hz}$ and $k_x = 78.5\ \mathrm{rad/m}$; and for the nonfluid-loaded plate, these values were $f = 2740\ \mathrm{Hz}$ and $k_x = 78.5\ \mathrm{rad/m}$. Note from Eqs. (58), (64), (65), (69), (75), and (76) that the displacement shape is contained entirely in the numerator and that the location of the mode in the wavenumber–frequency plane is contained entirely in the denominator. Additionally, because the single fluid-loaded plate contains no fluid terms in the numerator, it has a displacement

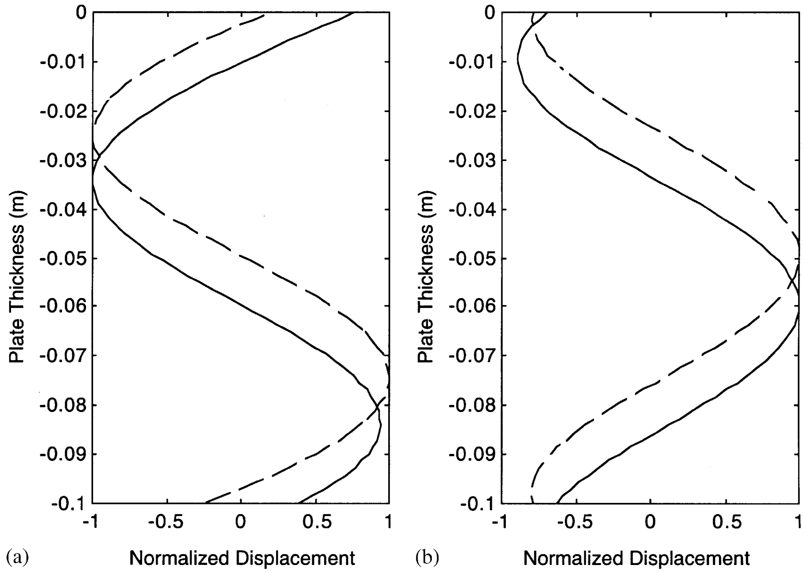

Fig. 2. Displacement shaper of the $n = 1$ mode in (a) tangential direction and (b) normal direction for the double fluid-loaded plate (———), single fluid-loaded plate and plate without fluid loading (– – – –).

shape identical to the nonfluid-loaded plate. However, the double fluid-loaded plate does contain fluid terms in the numerator, and thus its displacement shape is different from both the nonfluid-loaded plate and the single fluid-loaded plate. Comparison of displacement shapes at other modes yields similar results to those of the nonfluid-loaded, single-loaded, and double-loaded fluid plate displacement shapes shown in Fig. 2.

6. Conclusions

This paper has derived the closed-form solutions for a nonfluid-loaded, a single fluid-loaded, and a double fluid-loaded plate subjected to plane wave energy at all wavenumbers. The dispersion equation was also formulated based on the matrix equations and was verified using previously available dispersion equation forms. Furthermore, the displacement shapes of the system modes were determined, and it was found that the displacement shapes of the plate modes were identical for a nonfluid-loaded plate and for a single fluid-loaded plate. However, fluid loading on both sides produced a different displacement shape.

Acknowledgements

This work was funded by the Office of Naval Research. The author wishes to thank Karen Holt for her help with the technical-editing.

References

[1] A. Leissa, *Vibration of Plates*, American Institute of Physics, College Park, MD, 1973.
[2] H. Lamb, On waves in an elastic plate, *Proceedings of the Royal Society of London Series A* 93 (1917) 114–120.
[3] A. Freedman, The variation, with the Poisson ratio, of Lamb modes in a free plate, I: general spectra, *Journal of Sound and Vibration* 137 (2) (1990) 209–230.
[4] A. Freedman, The variation, with the Poisson ratio, of Lamb modes in a free plate, II: at transitions and coincidence values, *Journal of Sound and Vibration* 137 (2) (1990) 231–247.
[5] A. Freedman, The variation, with the Poisson ratio, of Lamb modes in a free plate, III: behaviour of individual modes, *Journal of Sound and Vibration* 137 (2) (1990) 249–266.
[6] M.F.M. Osborne, S.D. Hart, Transmission, reflection, and guiding of an exponential pulse by a steel plate in water, I: theory, *Journal of the Acoustical Society of America* 17 (1) (1945) 1–18.
[7] D.G. Crighton, The free and forced waves on a fluid-loaded elastic plate, *Journal of Sound and Vibration* 63 (2) (1979) 225–235.
[8] J. Dickey, G. Maidanik, H. Überall, The splitting of dispersion curves for the fluid-loaded plate, *Journal of the Acoustical Society of America* 98 (4) (1995) 2365–2367.
[9] A. Freedman, Effects of fluid loading on Lamb mode spectra, *Journal of the Acoustical Society of America* 99 (6) (1996) 3488–3496.
[10] X.L. Bao, H. Franklin, P.K. Raju, H. Überall, The splitting of dispersion curves for plates fluid loaded on both sides, *Journal of the Acoustical Society of America* 102 (2-pl) (1997) 1246–1248.
[11] K. Toda, K. Motegi, Coupling of velocity dispersion curves of leaky Lamb waves on a fluid-loaded plate, *Journal of the Acoustical Society of America* 107 (2) (2000) 1045–1048.

[12] J.H. Su, R. Vasudevan, On the radiation efficiency of infinite plates subjected to a point load in water, *Journal of Sound and Vibration* 208 (3) (1997) 441–455.

[13] W.A. Strawderman, *Wavevector–Frequency Analysis with Applications to Acoustics*, U.S. Government Printing Office, Washington, DC, 1996.

[14] J. Wu, Z. Zhu, The propagation of Lamb waves in a plate bordered with layers of a liquid, *Journal of the Acoustical Society of America* 91 (2) (1992) 861–867.

[15] M. Kim, Y.F. Hwang, An analysis of wave dispersion in coarsely laminated symmetric composite plates, *Journal of the Acoustical Society of America* 100 (4) (1996) 1981–1991.

[16] S.P. Timoshenko, J.N. Goodier, *Theory of Elasticity*, McGraw-Hill, New York, 1934.

[17] P.M. Morse, K.U. Ingard, *Theoretical Acoustics*, Princeton University Press, Princeton, NJ, 1968.

[18] M.C. Junger, D. Feit, *Sound, Structures, and Their Interaction*, MIT Press, Cambridge, MA, 1986.

[19] K.F. Graff, *Wave Motion in Elastic Solids*, Dover Publications, New York, 1975.